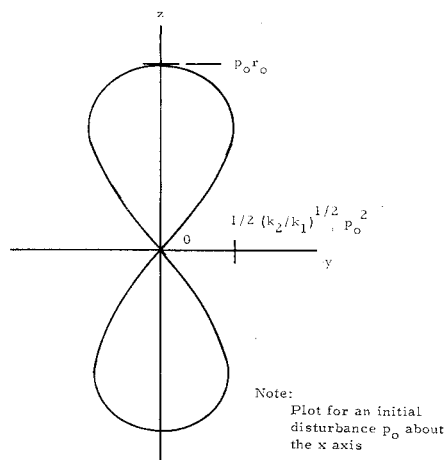
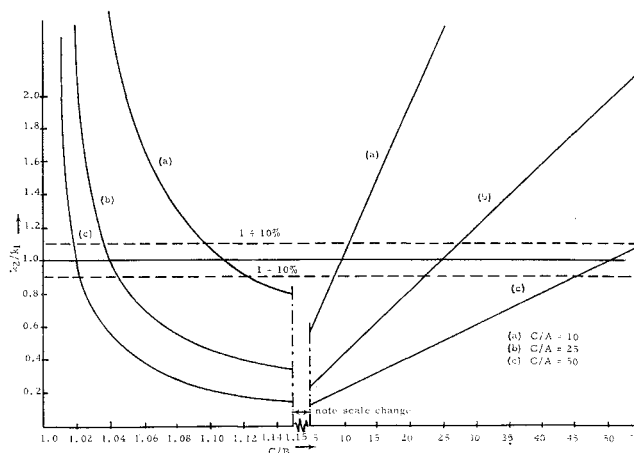
Fig. 2 Spin velocity variation vs γ .

An analysis of Eq. (8) shows that the field along each of the three body axes is oscillatory in direction and magnitude. Along the x axis, man's "down" direction, the resulting acceleration is composed of oscillatory components superimposed on the constant term, xr_0^2 . The accelerations perpendicular to the x axis given by the j and k terms give an interesting result when plotted (see Fig. 3). This figure shows that the gravity vector in the yz plane will vary in a "figure eight" with respect to man's down direction.

The characteristics of the oscillatory acceleration terms in Eq. (8) are directly related, both in magnitude and frequency, to the moment of inertia relationship of the rotating space station. In regard to magnitude, the ratio k_2/k_1 is plotted vs the ratio C/B for various C/A ratios in Fig. 4.

In this figure it is noted that for a given C/A value, the factor k_2/k_1 equals one for two different values of C/B and in between these values reduces to a minimum. An initial response to this result may be to select the minimum k_2/k_1 value of a selected C/A curve as defining a best configuration, but it should be noted that the ratio k_1/k_2 is an inverse function and will tend to magnify the magnitudes of the terms it affects with an end result of a greater fluctuation in the field than with $k_2/k_1 = 1$. Since it is desirable to reduce all acceleration component magnitudes simultaneously in order to reduce adverse effects to the man,² it is felt that $k_2/k_1 = 1 \pm 10\%$ should be the range selected initially for the moment-of-inertia relationship of a given configuration. The parameter K , which affects the oscillation frequency, increases in magnitude from the lower to higher value of C/B for a given C/A value, indicating that the period of oscillation is longer for a dumbbell than for a wheel configuration.

From the foregoing discussion, it is found that the constant magnitude and direction centrifugal force field normally associated with constant rotation about an axis transforms

Fig. 3 Gravity vector plot in yz plane.Fig. 4 k_2/k_1 vs C/B for various C/A values.

into a field of complex oscillatory magnitude and frequency characteristics when a space station exhibits disturbed rotational motion. In general, it was shown that these characteristics were dependent on the moment-of-inertia relationship for a given configuration. It is apparent that many other contingencies could be pursued but are beyond the scope of this report. Therefore, it is hoped that the analysis presented will at least serve to enlighten space station designers with the fact that man's physiological tolerance limits, especially those related to acceleration and frequency changes, must be carefully considered in the selection of artificial gravity space station design parameters.

References

- Page, L., *Introduction to Theoretical Physics* (D. Van Nostrand Co., Inc., Princeton, N. J., 1935), 2nd ed., Chap. II, Sec. 42.
- Guedry, F. E. and Richmond, G., "Differences in response latency with different magnitude angular accelerations," U. S. Army Medical Research Lab. Rept. 301, Fort Knox, Ky. (November 1957).

Umbra and Penumbra Eclipse Factors for Satellite Orbits

SOL ZALEL FIXLER*

Republic Aviation Corporation, Farmingdale, N. Y.

A. Introduction

THE amount of time a satellite is occulted by the earth shadow during an orbit is of major consequence in determining the satellite thermal control system, the power supply (if powered by a solar source), and the atmospheric control system. To a lesser extent, the satellite external torque history and the sensor systems are also influenced by the time the satellite spends in the earth shadow.

B. Physics of the Problem

The earth shadow consists of two regions, the umbra and the penumbra, as shown in Fig. 1. The umbra is the conical total shadow projected from the earth on the side opposite the sun. In this region, the solar radiation intensity is zero. The penumbra is the partial shadow between the umbra and the full-light region. In the penumbra, the light of the sun is only

Received December 23, 1963; revision received April 28, 1964.

* Specialist Thermodynamics Engineer, Space Systems Division. Member AIAA.

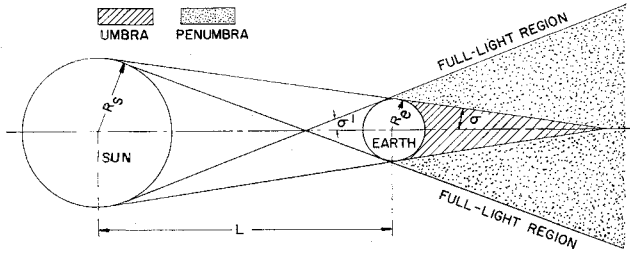


Fig. 1 Earth umbra and penumbra relationships.

partially cut off by the earth. The solar radiation intensity within the penumbra region varies from its full value at the border of the full-light region to zero at the umbra border.

The reduction in solar radiation intensity in the penumbra region is due to the partial blockage by the earth of the sun's disk. If the distribution of energy over the sun's disk were uniform, the intensity at any point in the penumbra would be directly proportional to the area of the sun's disk that is not blocked by the earth. In actuality, the energy distribution over the sun's disk is not uniform.

C. Limitations of Previous Work

In the existing literature on the subject, most authors¹⁻⁴ assume a cylindrical earth shadow, which results in an inexact solution. Reference 5 treated the earth shadow as a cone, but did not analyze the effects of the penumbra. For low-altitude orbits, these simplifications introduce small errors and are probably justified in view of the more complicated analysis required for an exact solution. However, for highly elliptical orbits (or high altitude circular orbits) with apogees extending to synchronous altitudes and beyond, the approximation of a conical shadow by a cylinder can lead to gross errors in the calculated shadow times.

D. Analysis

In the analysis to follow, the earth is assumed to be a sphere of equatorial radius and the center of an inverse-square central force field. The refractive effect of the earth's atmosphere on the sun's rays was not investigated rigorously in this study. However, the effect can be accounted for by changing the semivertex angle of the shadow cone once the cone contraction due to atmospheric refraction is established.

1. Umbra eclipse factor

The umbra eclipse factor is defined as the ratio of the time a satellite is occulted by the earth umbra to the time of a complete satellite orbit and is given by

$$\epsilon_u = (t_2 - t_1)/P \quad (1)$$

where

ϵ_u = umbra eclipse factor

t_1 = time (measured from perigee) when the satellite enters the umbra cone

t_2 = time (measured from perigee) when the satellite emerges from the umbra cone

P = orbital period

The time difference between umbra entrance and exit, $t_2 - t_1$, in Eq. (1) can be determined by Kepler's law, resulting in an expression for ϵ_u given by

$$\epsilon_u = \frac{e(1-e^2)^{1/2}}{2\pi} \left[\frac{\sin(\phi_1 - \alpha)}{1 + e \cos(\phi_1 - \alpha)} - \frac{\sin(\phi_2 - \alpha)}{1 + e \cos(\phi_2 - \alpha)} \right] + \frac{1}{\pi} \left\{ \tan^{-1} \left[\left(\frac{1-e}{1+e} \right)^{1/2} \times \tan \left(\frac{\phi_2 - \alpha}{2} \right) \right] - \tan^{-1} \left[\left(\frac{1-e}{1+e} \right)^{1/2} \tan \left(\frac{\phi_1 - \alpha}{2} \right) \right] \right\} \quad (2)$$

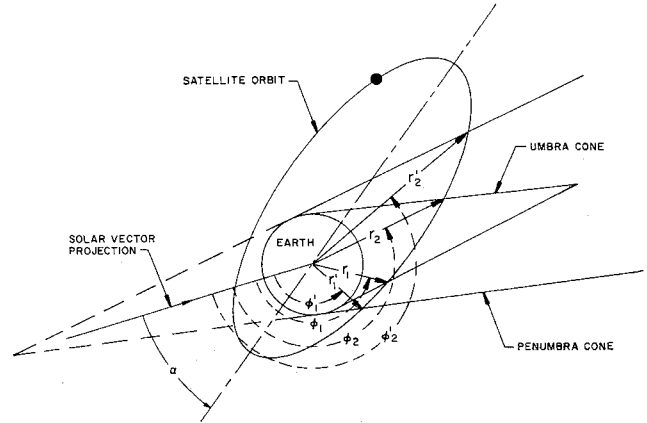


Fig. 2 Geometry for the satellite orbit, earth umbra, and penumbra.

where

e = eccentricity of the orbit

ϕ_1 = angle swept out by radius vector at time t_1

ϕ_2 = angle swept out by radius vector at time t_2

α = reference angle from which ϕ is measured

The reference angle α is defined as the angle formed by the major axis (at the point of perigee) and the projection of the solar vector on to the orbital plane as shown in Fig. 2. If we define γ as the angle between the orbital plane and the solar vector, the orientation of the orbit in space can be completely defined by specifying α and γ . The fact that α is undefined when $\gamma = \pi/2$ is of no consequence since, when $\gamma = \pi/2$, the satellite orbit is 100% sunlit and the eclipse factor is zero.

The last equation gives the umbra eclipse factor in terms of the known quantities e , α and the unknown angles ϕ_1 , ϕ_2 corresponding to the points where the satellite enters and leaves the umbra, respectively. In order to determine ϕ_1 and ϕ_2 in terms of known quantities, the following analysis is presented. In Fig. 3a, AB is the orbital plane on edge showing γ , the angle between the solar vector and the orbital plane, in true size. CD is a plane normal to the solar vector. Figure 3b shows the orbital plane rotated 90° (counterclockwise, viewed from B to A) about the projection of the solar vector on to the orbital plane. The components of r_1 (the radius vector at the point of umbra entry) ln and lm , normal and parallel to the solar vector projection are shown in terms of ϕ_1 . The projection of these components on plane CD are shown in Fig. 3c as $l'n'$ and $l'm'$. Since triangle $l'm'n'$ is a right triangle, the following is true:

$$\left[r_1 \sin \left(\phi_1 - \frac{\pi}{2} \right) \sin \gamma \right]^2 + \left[r_1 \cos \left(\phi_1 - \frac{\pi}{2} \right) \right]^2 = (m'n')^2 \quad (3)$$

Point m' is on the cone of the umbra, and therefore $m'n'$ is the projection of r_1 on plane CD , giving

$$m'n' = r_1 \cos \Omega \quad (4)$$

where Ω is the angle that r_1 makes with plane CD (perpendicular to solar vector) and is given by

$$\Omega = \sin^{-1} \left\{ \frac{1}{r_1} [R_e \sin \sigma + \cos \sigma (r_1^2 - R_e^2)^{1/2}] \right\} \quad (5)$$

where R_e is the earth radius, and σ is the umbra half-cone angle given by

$$\sigma = \sin^{-1} \left[\frac{R_s}{L} \left(1 - \frac{R_e}{R_s} \right) \right] \quad (6)$$

R_s being the sun radius and L the astronomical unit (see Fig. 1). Combining Eqs. (3-5), we get

$$\cos^2 \phi \cos^2 \gamma = \left\{ \frac{1 + e \cos(\phi - \alpha)}{a(1 - e^2)} \times \left[R_s \sin \sigma + \cos \sigma \left(\left[\frac{a(1 - e^2)}{1 + \cos(\phi - \alpha)} \right] - R_s^2 \right)^{1/2} \right] \right\}^2 \quad (7)$$

where the satellite orbit, in plane polar coordinates, was assumed to be given (neglecting perturbation effects) by

$$r = \frac{a(1 - e^2)}{1 + e \cos(\phi - \alpha)} \quad (8)$$

a being the semimajor axis of the orbit.

Subscript 1 was omitted in (7) and (8), since a similar expression to (7) can be obtained by repeating the development in Fig. 3 for r_2 , the radius vector at the point where the satellite leaves the umbra. In that case, Eq. (7) would be given in terms of ϕ_2 instead of ϕ_1 .

There are four distinct roots (for ϕ) to Eq. (7). Since the umbra is displaced 180° from the solar vector projection (see Fig. 2), the only pertinent roots are those in the second and third quadrant. These roots correspond to umbra entry and exit, respectively. (Recall that ϕ is measured from the solar vector projection.) For a given α , γ and orbital elements e and a , we can determine ϕ_1 and ϕ_2 from Eq. (7) by the following criteria:

$$\phi = \phi_1 \text{ if } \pi > \phi > \pi/2 \quad (9)$$

$$\phi = \phi_2 \text{ if } 3\pi/2 > \phi > \pi \quad (10)$$

The umbra eclipse factor ϵ_u can then be found from Eq. (2).

2. Penumbra eclipse factor

The analysis for the penumbra eclipse factor is similar to that of the umbra eclipse factor. The penumbra eclipse factor is defined as the ratio of the time a satellite is occulted by the earth penumbra to the time of a complete satellite orbit and is given by

$$\epsilon_p = \epsilon_u(\phi'_1, \phi'_2) - \epsilon_u(\phi_1, \phi_2) \quad (11)$$

where $\epsilon_u(\phi_1, \phi_2)$ is obtained from Eq. (2) evaluated at ϕ_1 and

ϕ_2 , and $\epsilon_u(\phi'_1, \phi'_2)$ is obtained from Eq. (2) evaluated at ϕ'_1 and ϕ'_2 (see Fig. 2). The angles ϕ'_1 and ϕ'_2 are obtained from Eq. (7) in the same manner as ϕ_1 and ϕ_2 , except that σ is replaced by $-\sigma'$ where σ' is the penumbra half-cone angle (see Fig. 1) and is given by

$$\sigma' = \sin^{-1} \left[\frac{R_s}{L} \left(1 + \frac{R_e}{R_s} \right) \right] \quad (12)$$

E. Computing Program

The method described previously for calculating umbra and penumbra eclipse factors lends itself to a straightforward hand calculation. The only difficult step is the solving of Eq. (7), which is transcendental and requires assumptions and iterations. To avoid this difficulty, the analysis was programmed for, and results for a number of orbits computed on, the IBM 7090 computer. The required variable inputs are α , γ , h_a , and h_p , where h_a is the apogee altitude and h_p is the perigee altitude. The fixed inputs are σ , σ' , and R_s . Their respective values, as used in the computations, are 0.00461715 rad, 0.00470245 rad, and 3,441.845 naut miles. The quantities e and a are related to h_a and h_p by

$$e = (h_a - h_p)/(2R_e + h_a + h_p) \quad (13)$$

$$a = [(h_a + h_p)/2] + R_e \quad (14)$$

The average running time to compute both the umbra and penumbra eclipse factors for a given orbit was approximately 0.2 sec.

References

- 1 Stoddard, L. G., "Eclipse of artificial earth satellite," *Astronaut. Sci. Rev.* **III**, 9-16 (April-June 1961).
- 2 Pierce, D., "A rapid method for determining the percentage of a circular orbit in the shadow of the earth," *Astronaut. Sci.* **IX**, 89-92 (Fall 1962).
- 3 Patterson, G. B., "Graphical method for prediction of time in sunlight for a circular orbit," *ARSJ.* **31**, 441-442 (1961).
- 4 Cunningham, F. G., "Calculation of the eclipse factor for elliptical satellite orbits," NASA TN D-1347 (1962).
- 5 Peckham, G. W., "The orbital shadow time of an earth satellite," Institute of Technology, Air Univ., U. S. Air Force, GAE/AE-60-9 (1960).

Exact Kinetic and Approximate Nozzle Recombination Losses

DAVID MIGDAL* AND ARNOLD GOLDFORD†

Grumman Aircraft Engineering Corporation, Bethpage, N. Y.

APPROXIMATE losses due to a nonequilibrium nozzle flow recently have been investigated for space rocket engines and hypersonic ramjets.^{1,2} Although formal methods are available for a multicomponent system,^{3,4} such analyses require extensive computer time. The approximate method of Ref. 1 utilizes Bray's criterion⁵ to predict a freezing point where the rate of change of total number of moles required for equilibrium is equal to the recombination rate. This procedure appears to compare well with the exact analyses of Refs. 3 and 4 and some experimental data.⁶

In the approximate method,¹ the equilibrium rate of change is computed as follows:

$$Q = V \frac{d(\Sigma n_i)}{d(A/A^*)} \frac{d(A/A^*)}{dl}$$

Received December 30, 1963; revision received March 16, 1964.

* Senior Gas Dynamics Engineer. Member AIAA.

† Senior Propulsion Engineer. Member AIAA.

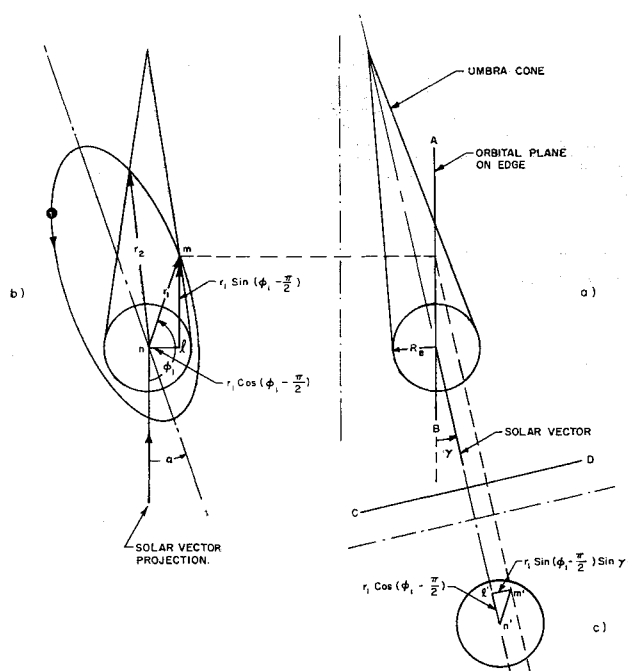


Fig. 3 Geometry for the determination of umbra eclipse factor.